Hindawi
International Journal of Antennas and Propagation
Volume 2022, Article ID 8679798, 10 pages
https://doi.org/10.1155/2022/8679798

Research Article

Design a Multistub Array Antenna at 28 GHz with Beam Switching Ability

A. Lak

Department of Electrical Engineering, Genaveh Branch, Islamic Azad University, Genaveh, Iran

Correspondence should be addressed to A. Lak; lak.asmae@gmail.com

Received 17 August 2022; Revised 8 October 2022; Accepted 19 October 2022; Published 1 November 2022

Academic Editor: Mohammad Alibakhshikenari

In this paper, a Millimeter Wave antenna is designed which has a compact, lightweight and planar configuration. The frequency band is 27–29.5 GHz as a candidate band for 5G/millimeter Wave (mmW) systems. The antenna structure is similar to Quasi Yagi antenna which has driver, director, feeding part, and reflector. Substrate Integrated Waveguide used for feeding part of single element antenna and Wilkinson power divider used for antenna array feeding network. The proposed antenna has been simulated, fabricated, and measured (S11, *E*, and *H* pattern). The simulation and measurement values showed good similarity. The switched line phase shifter used to consider the beam steering (rotation) ability of the designed antenna which is important in (mmW) systems such as RADARs and mobile handsets. To evaluate this ability, for **0**°, **30**°, **45**°, and **90**° phase differences, the beam steering angle (θ) simulated and also for **−90**° and **90**° implemented. The results showed that the efficiency, S11, and *E* patterns in the rotated beam is suitable and without degradation in antenna operation. To simulate and evaluate the designed antenna HFSS and CST Software are used.

1. Introduction

Today the mobile communication service is an essential part of human life. Many researchers all of the world work on electromagnetic fields and their applications. Because of increasing demands for higher data rates (such as wireless broadband connections, massive machine type communications, and highly reliable networks), the research studies on fifth-generation (5G) mobile communication systems have started. The standardization of this technology is coming in 2020s [1, 2]. Compared with previous generations, 5G mobile communication networks will use broader frequency bandwidths. One of the candidate frequencies for this band is 28 GHz (27–29.5 GHz). The other frequency bands can be seen in [3]. In this paper, 28 GHz has been selected because of fabrication considerations. Many types of antenna are used in Millimeter wave band such as Fermi, Vivaldi, and Quasi Yagi [4–6].

Quasi-Yagi is an interesting antenna because of its benefits, such as simple structure, lightweight, and easy forming array. So, in this paper, the Quasi-Yagi is selected as base of the proposed antenna [7].

Single element antenna has a small gain to prevail the path loss at mmW band. According to Friis equation, by increasing the frequency, the signal wavelength becomes shorter and consequently the free-space path loss becomes higher [8].

The array antenna can solve this problem by increasing the gain. Also, it has higher directivity, reduces minor lobes, and shows better performance rather than a single element [9].

The structure of the proposed antenna is based on Quasi-Yagi, which consists of dipole elements, directors, reflectors, and feeding part.

In some 5G devices and systems, it needed to change the main beam direction as the array gain compensates for the small antenna aperture and the large noise bandwidth. Beam steering is a technique for changing the direction of the main beam of a radiation pattern. Also, it is a way to control the field distribution [10, 11]. This technique is very important

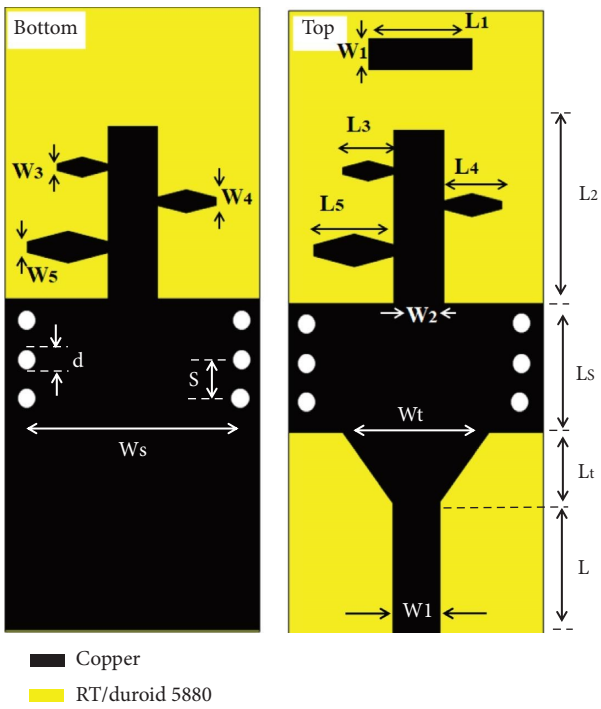

Figure 1: The structure of the proposed antenna.

in mmW or 5G systems like cellphones and RADARs to have a good quality in communication.

In the previous author's job [12], three single element antennas have been designed, simulated, and fabricated. Also, in [13] three array antenna have been designed, simulated and one of them fabricated. All of them had good characteristics such as enough gain, end fire pattern, and good S_{11} to use in 5G mobile handsets (27–29.5 GHz).

In this paper, according to one of the proposed antenna structure in [12] a phased array antenna is designed and the beam steering (rotating) property of the designed array antenna is simulated and implemented in the software. The array antenna consists of eight single elements. The feeding part of the array is Wilkinson power divider (WPD) because of its benefits. To evaluate the WPD performance three parameters should be checked: refection coefficients, coupling, and isolation between ports [14] which are considered in [13]. The switched line phase shifter is used to create the required phase difference.

In the following sections, the design and simulation process is described. According to the obtained results of the proposed antenna (i.e., compact size, beam steering, and other good characteristics) it can be considered as good candidates for mmW/5G devices.

2. Antenna Design

As mentioned in introduction part in this paper Quasi Yagi structure is used because of its benefit such as its light-weight, planar structure, and low cost which is an ideal structure to apply in handheld devices. In consonance with Quasi Yagi antenna structure, the proposed antenna has a feeding part, director, driver, and reflector. To design the feeding part of single element antenna, SIW (Substrate Integrated waveguide) technology is used. SIW is a compact, low-loss, and cost effectiveness structure. The substrate is Roger RT/duroid 5880 with $\varepsilon_r = 2.2$ and $h_{sub} = 0.38$ mm. The phase difference between the up and down plane of the substrate.

is 180° and a 50 Ω lumped port is used for the port excitation. Based on the antenna feed system in Figure 1, the TE_{10} mode is excited. To calculate the SIW parameters and transition part of the feeding network equations (1)–(4) are used.

$$d < s < 2d, \tag{1}$$

$$w = \frac{c}{2f_c\sqrt{\varepsilon_r}}, \tag{2}$$

$$W_T \approx 0.4w, \tag{3}$$

$$\lambda g/2 < L_T < \lambda g, \tag{4}$$

where w is the width of waveguide, w_t is the width of taper, Lt is the length of taper, Ls is the length of SIW part, s is the distance between two adjacent vias, d is the diameter of via, and L_T is the length of taper. So for TE_{10} mode, these parameters are equal to the following variables.

$Ls = 3.5\ mm, W_T = 3.2\ mm,\ L = 3.5\ mm,\ w = 5.5\ mm, L_T = 1.6\ mm,\ d = 0.6\ mm,\ s = 1.2\ mm.$ More detail of SIW calculations are in [15, 16].

Single element antenna does not have enough gain to overcome the pass loss. There are some methods to increase the gain of antenna, for example using of the array antenna. Thus the array antenna is used. For the radiation part the log periodic antenna structure is applied which is endfire, has good gain, and smaller size rather than other structures such as Fermi, Cavity backed, and Vivaldi. For the log periodic antenna, the lengths (L) and widths (w) of adjacent elements are calculated as follows [17]:

$$\tau = \frac{L_{m+1}}{L_m} = \frac{W_{m+1}}{W_m}, \tag{5}$$

$$\varepsilon_{eff} = \left(\frac{\varepsilon_r + 1}{2}\right) + \frac{((\varepsilon_r - 1))}{2}\left(1 + 12\left(\frac{h}{w}\right)^{-0.5}\right), \tag{6}$$

$$L_1 = \lambda_{effmax}/4 = c/4\sqrt{\varepsilon_{eff}}f_{\min}, \tag{7}$$

where λ_{eff} is the effective wavelength, h is the thickness of substrate and w is the width of the longest element. The number of elements (N) is determined as follows:

$$\sigma = \frac{(1-\tau)}{4\tan\alpha}, \tag{8}$$

$$N = 1 + \frac{(\ln(B_{AR} \times B)}{\ln(1/\tau))}, \tag{9}$$

$$B = \frac{f_{\max}}{f_{\min}}, \tag{10}$$

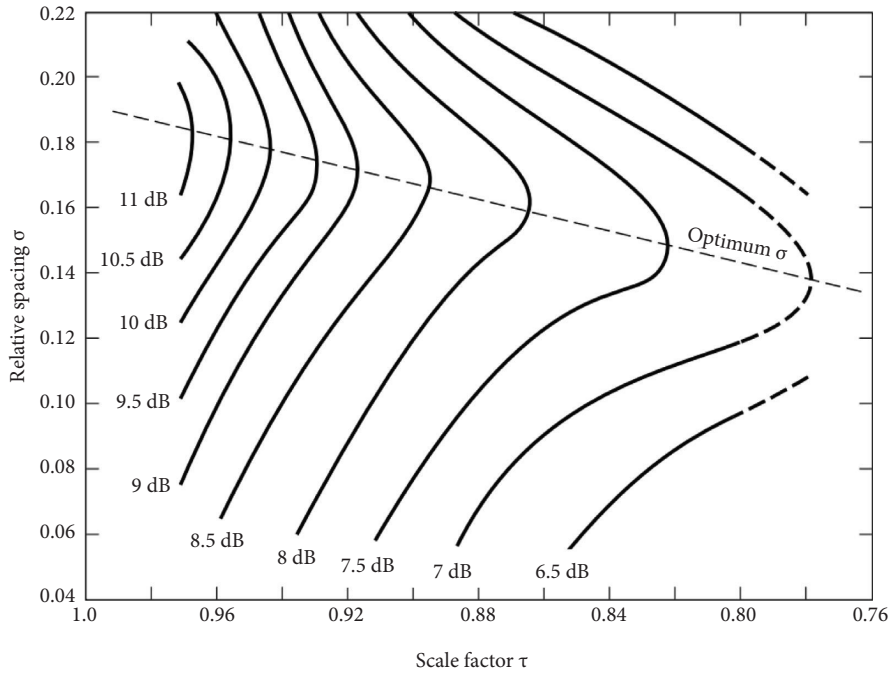

Figure 2: Computed contours of constant directivity versus σ and τ for log-periodic dipole arrays.

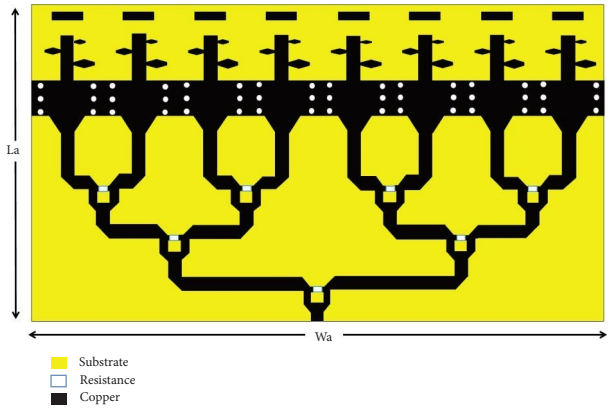

Figure 3: Antenna array structure.

$$B_{AR} = 1.1 + 7.7\,(1-\tau)^2 \cot\alpha, \tag{11}$$

where σ is the spacing factor, α is the apex angle, τ is the geometry constant, and B_{AR} is the bandwidth of the active region.

For 7 dB gain in Figure 2, scale factor (τ) and Relative spacing (σ) are 0.78 and 0.131, respectively. By using of these parameters in equations 5 to 11 the other parameters are calculated. So the number of elements is $N = 3$. Figure 3 shows the structure of the antenna.

According to Figure 1, the calculated dimension are $L_1 = 2.8$ mm, $L_2 = 4.22$ mm $L_3 = 1.068$ mm, $L_4 = 1.425$ mm, $L_5 = 1.9$ mm, $W_1 = 0.75$ mm, $W_2 = 1.25$ mm, $W_3 = 0.14$ mm, $W_4 = 0.1875$ mm, and $W_5 = 0.25$ mm.

The antenna array is consisting of eight single elements and an eight way Wilkinson Power Divider (WPD) as a feeding network as shown in Figure 3. In two-way WPD, the isolation resistor is $2Z_0$ and the impedance of $\lambda/4$ is $\sqrt{2}Z_0$. For equal WPD the $Z_0 = 50\ \Omega$, the impedance of $\lambda/4$ is $\sqrt{2}Z_0 = 70.7\ \Omega$ and isolation resistor is $2Z_0 = 100\ \Omega$. To design WPD at 28 GHz the TXline calculator is used. The values for WPD are obtained as: $W_{50\Omega} = 1.18$ mm, $W_{70.7\Omega} = 0.65$ mm, and $L_{70.7\Omega} = 1.97$ mm. The isolation resistor is 100 Ω (size is $1 \times 0.5\ \text{mm}^2$) from 0402 SMD family. For eight ways of WPD, three stages of two ways WPD is needed [13]. The antenna array with feeding network (WPD) is shown in Figure 3. In an antenna array, the distance between elements is about 0.5λ to control mutual coupling.

The fabricated prototypes of the proposed antennas are shown in Figure 4.

Measurement and simulation results of antenna array (S_{11}, Normalized E and H patterns) are shown in Figure 5.

There is some difference between measured and simulated results because of SMK losses, fabrication faults, resistors etc. The overall antenna size of a single element and array are 6.5 mm × 18 mm × 0.38 mm and 52 mm × 29.96 mm × 0.38 mm, respectively, which are suitable for hand held devices.

The maximum gain of a single element is 8 dBi and array is 14.6 dBi respectively. The E and H patterns are end fire and S_{11} coefficient values are under −10 dB. More gains can be reached by increasing the number of directors, but it increases the size of the antenna. All of these characteristics show that the proposed antenna is suitable for mmW/5G applications.

In [13] the Specific Absorption Rate of the antenna was evaluated. A three layers human head model situated in a 5 mm distance from the antenna. The power of the antenna was 15 and 20 dBm according to 5G standard values. The results showed that all of the SAR values are in standard range (i.e., 1.6 W/Kg according to FCC standard).

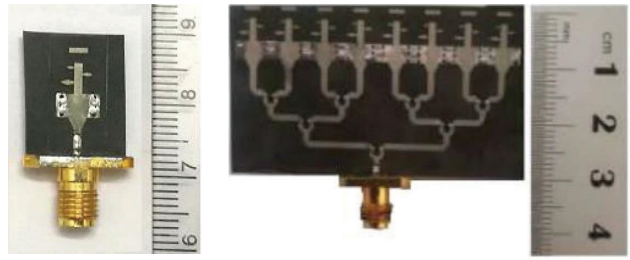

(a) (b)

Figure 4: (a) Single element. (b) Antenna array [13].

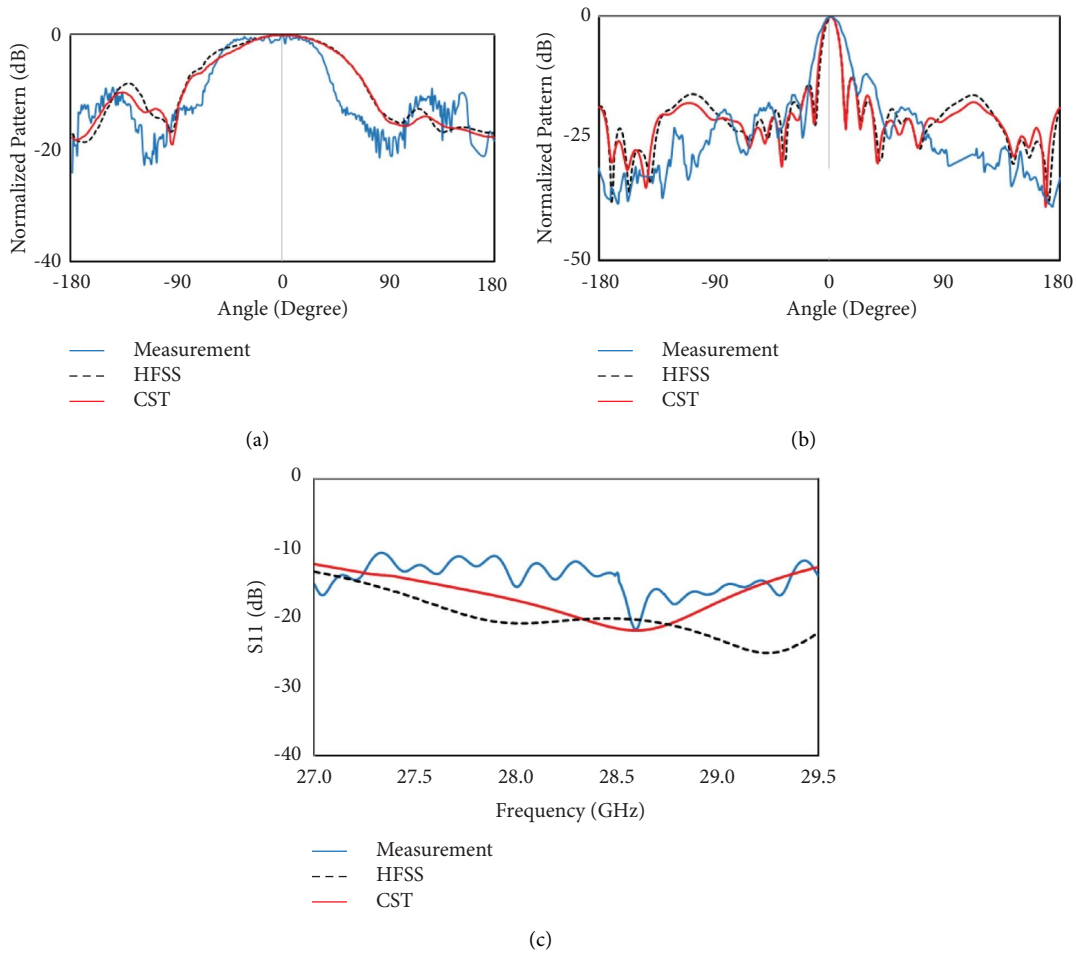

Figure 5: (a) Normalized H pattern, (b) Normalized E-pattern, and (c) S_{11} coefficient of the proposed antennas at 28 GHz; [13].

3. Linear Phased Array Antenna

3.1. Introduction. To better covering the space losses in the communication process the beam steering methods can be used by creating the phase difference. In this part the rules of designing phased array antenna is presented.

Figure 6 shows a linear phased array antenna with K elements and equally spaced by a distance d. The direction of a wave is described by the angle θ between rays and the array normal. According to Figure 6 the array radiation pattern is written by (12).

$$S(\theta) = \sum_{i=1}^{K} S_i(\theta) = (S)_e(\theta)).(S_a(\theta)) = (S_e(\theta)) \sum_{i=1}^{K} a_i e^{j[K_0(K-i)\mathrm{d} \quad \sin\ (\theta)+\psi_i]}, \tag{12}$$

where S_e is the element radiation pattern, S_a is array factor, ψ_i is the phase difference, K is the number of elements, and K_0 is the free-space wave number. All the coefficients a_i form an amplitude taper. Let us assume a

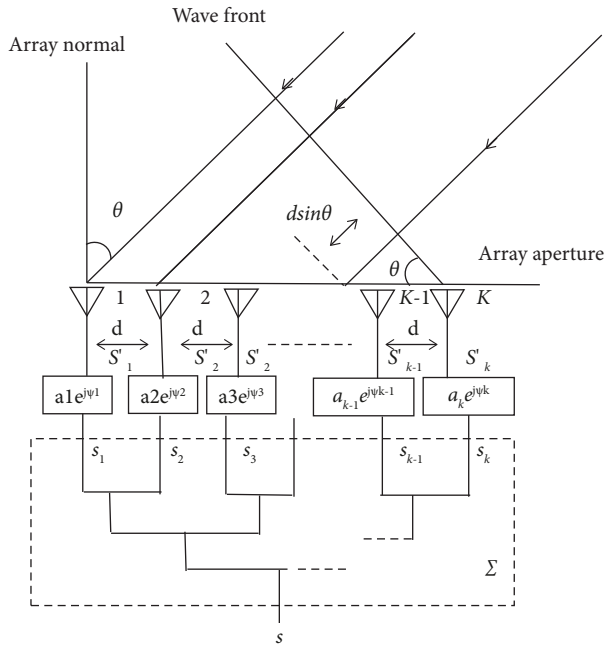

Figure 6: A linear phased array of K radiators[11].

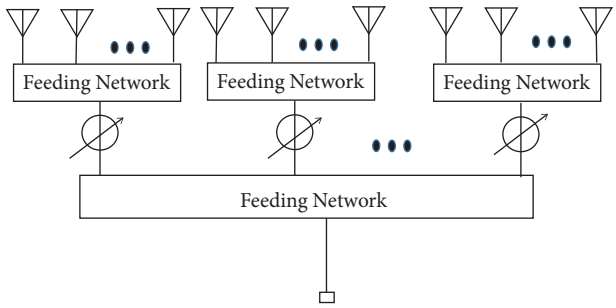

Figure 7: Grouping antennas into a sub-array [18].

uniform, normalized amplitude distribution, so for K elements:

$$a_i = 1, \mathrm{i} = 1, 2, \ldots, \mathrm{K}. \tag{13}$$

So only S_a is considered. If a linear phase taper is chosen:

$$\psi_i = k_0 (K - i)d \quad \sin(\theta_0), -90 < \theta_0 < 90. \tag{14}$$

Since $-90 < \theta_0 < 90$, the array factor may be written as follows:

$$S_a(\theta) = \sum_{i=1}^{K} e^{jk_0(K-i)d[\sin(\theta)-\sin(\theta_0)]}. \tag{15}$$

For the linear phased array antenna situation, maximum array factor is $\theta = \theta_0$ from (16).

$$\sin(\theta) - \sin(\theta_0) = 0. \tag{16}$$

So by choosing θ_0 in $\psi_i = k_0 (K - i)d \sin(\theta_0)$ the array factor will have its maximum at θ_0.

A phased array antenna is a complicated structure in designing and fabrication thus, reduction of complexity, cost, and size is very important to use in more devices specially handhelds. Create several subarrays within the antenna which each group is controlled by a phase-shifter reduces the number of phase-shifters and the cost. Each group is seen as a single element to other groups (Figure 7).

In this paper to reach enough gain at mmW frequency bands (to overcome the path losses), eight elements are used which are arranged linearly with about 0.5 λ distance between them. In Figure 8-show the antenna array and subarrays. In this case the spacing between two elements is around 1.1λ because two elements are combined and assumed as one element according to Figures 7, 8(a), and 8(b).

3.2. Phase Difference. There are several phase shifters like Switched Line Phase Shifters, Loaded Line phase shifters, High-Pass/Low- Pass phase shifter, and Quadrature phase shifter. In this paper, Switched Line Phase Shifters (Figure 9) is used because of the simplest configuration and it provides a good insight into the concept behind phase shifters. Also, this method has certain advantages over other phase shifters as φ is a linear function of frequency and independent of time and temperature changes since it solely depends on the length of the transmission lines [19].

By creating a time delay difference between two paths (changing the length of L with respect to L_0) the desired phase shift can reach in the transmission line. All of the diodes are assumed as an ideal diode.

Reference line is L_0 and the delay line length is L_0+L. Different path lengths which result in a phase delay (φ) [18, 20–22]. As mentioned above, to design the beam switching network of the array antenna, the switched line phase shifter is used. For a desired beam direction (θ) in Figure 8(b) it is necessary to create the related phase shift by using equations (17)–(20).

$$\mathrm{L}_0 = \frac{\lambda}{\sqrt{\varepsilon_{\mathrm{eff}}}}\left(1 - \frac{0}{2\pi}\right), \tag{17}$$

$$\mathrm{L}_1 = \frac{\lambda}{\sqrt{\varepsilon_{\mathrm{eff}}}}\left(1 - \frac{\varphi}{2\pi}\right), \tag{18}$$

$$\mathrm{L}_2 = \frac{\lambda}{\sqrt{\varepsilon_{\mathrm{eff}}}}\left(1 - \frac{2\varphi}{2\pi}\right), \tag{19}$$

$$\mathrm{L}_3 = \frac{\lambda}{\sqrt{\varepsilon_{\mathrm{eff}}}}\left(1 - \frac{3\varphi}{2\pi}\right). \tag{20}$$

And, for φ calculate from (21).

$$\varphi = \left(\frac{2\pi}{\lambda}\right)\mathrm{d}\sin(\theta). \tag{21}$$

3.3. Calculations. In this paper, the calculations for the favorite (selective) phase shift $\varphi = 0^\circ, 30^\circ, 45^\circ, 90^\circ$, and -90° and associated beam direction (θ) are done. For example for $\varphi = 30^\circ$, since at 28 GHz, $\lambda = 10.7mm$ and taking into account to substrate characteristic $\varepsilon_{\mathrm{eff}} = 1.87$, from (13) to (17) θ can be found as follows:

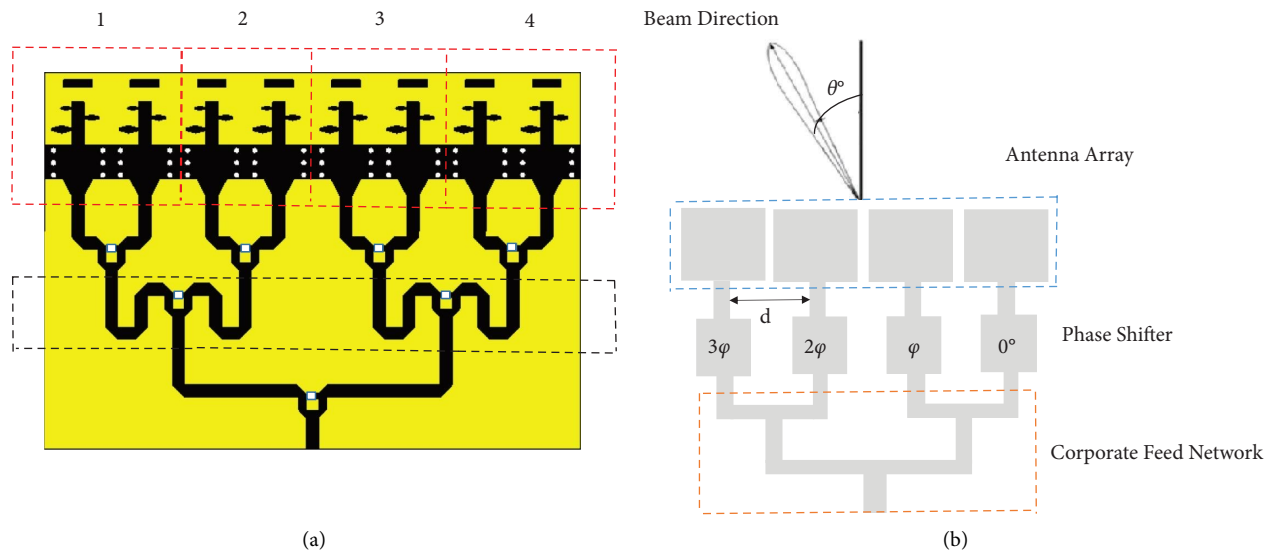

Figure 8: (a) Eight elements array with 0 degree phase difference, (b). Four sub arrays.

Table 1: Calculations for 30°, 45°, and 90°

φ (degree)	L_0 (mm)	L_1 (mm)	L_2 (mm)	L_3 (mm)	θ (degree)
30	7.86	7.21	6.55	5.89	3.94
45	7.86	6.33	5.42	4.51	6
90	7.86	5.89	3.93	1.96	11.9

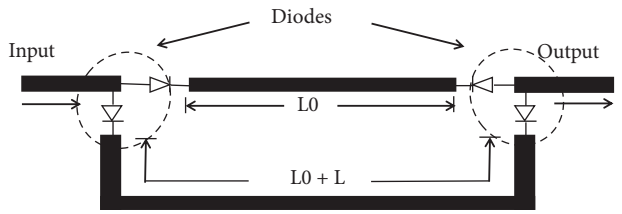

Figure 9: Basic schematic of phase shifter operation using diodes [19].

$$L_0 = \frac{10.7}{\sqrt{1.87}}\left(1 - \frac{0}{360^\circ}\right) = 7.86\text{mm},$$

$$L_1 = \frac{10.7}{\sqrt{1.87}}\left(1 - \frac{30^\circ}{360^\circ}\right) = 7.21\text{mm},$$

$$L_2 = \frac{10.7}{\sqrt{1.87}}\left(1 - \frac{60^\circ}{360^\circ}\right) = 6.55\text{mm}, \quad (22)$$

$$L_3 = \frac{10.7}{\sqrt{1.87}}\left(1 - \frac{30^\circ}{360^\circ}\right) = 5.89\text{mm},$$

$$\theta = \sin^{-1}(\varphi * \lambda/2\pi\, d) = \sin^{-1}\left(\frac{(\pi/6)\lambda}{2\pi * 1.21\lambda}\right) = 3.94^\circ.$$

Table 1shows the calculations for 30, 45, 90, and -90 degrees.

4. Simulation

By the calculated parameters from Table 1 antenna array is simulated in Figure 10. This figure shows the results of the simulation for 30°, 45°, and 90° phase differences and corresponding beam direction (θ). Figure 10(a) shows the phase difference 30° ($\theta = 4^\circ$), and Figures 10(d), 10(g), and 10(j) are the results of normalized E-pattern with respect to 0° phase difference, S_{11} and efficiency of this state respectively. Figure 9(b) shows the phase difference 45° ($\theta = 7^\circ$) and Figures 10(e), 10(h), and 10(k) are the results of normalized E-pattern with respect to 0° phase difference, S_{11} and efficiency of this state respectively. Figure 10(c) shows phase difference 90° ($\theta = 11^\circ$), and Figures 10(f), 10(i), and 10(l) are the results of normalized E-pattern with respect to 0° phase difference, S_{11} and Efficiency of this state respectively. As it can be seen the results of simulation are in agreement with the values from calculations. As the results show, in all cases the efficiency, S_{11} and pattern are suitable and without any degradation in antenna performance. Figure 11 presents the beam steering at 0°, 30°, 45°, and 90° phase differences in one chart.

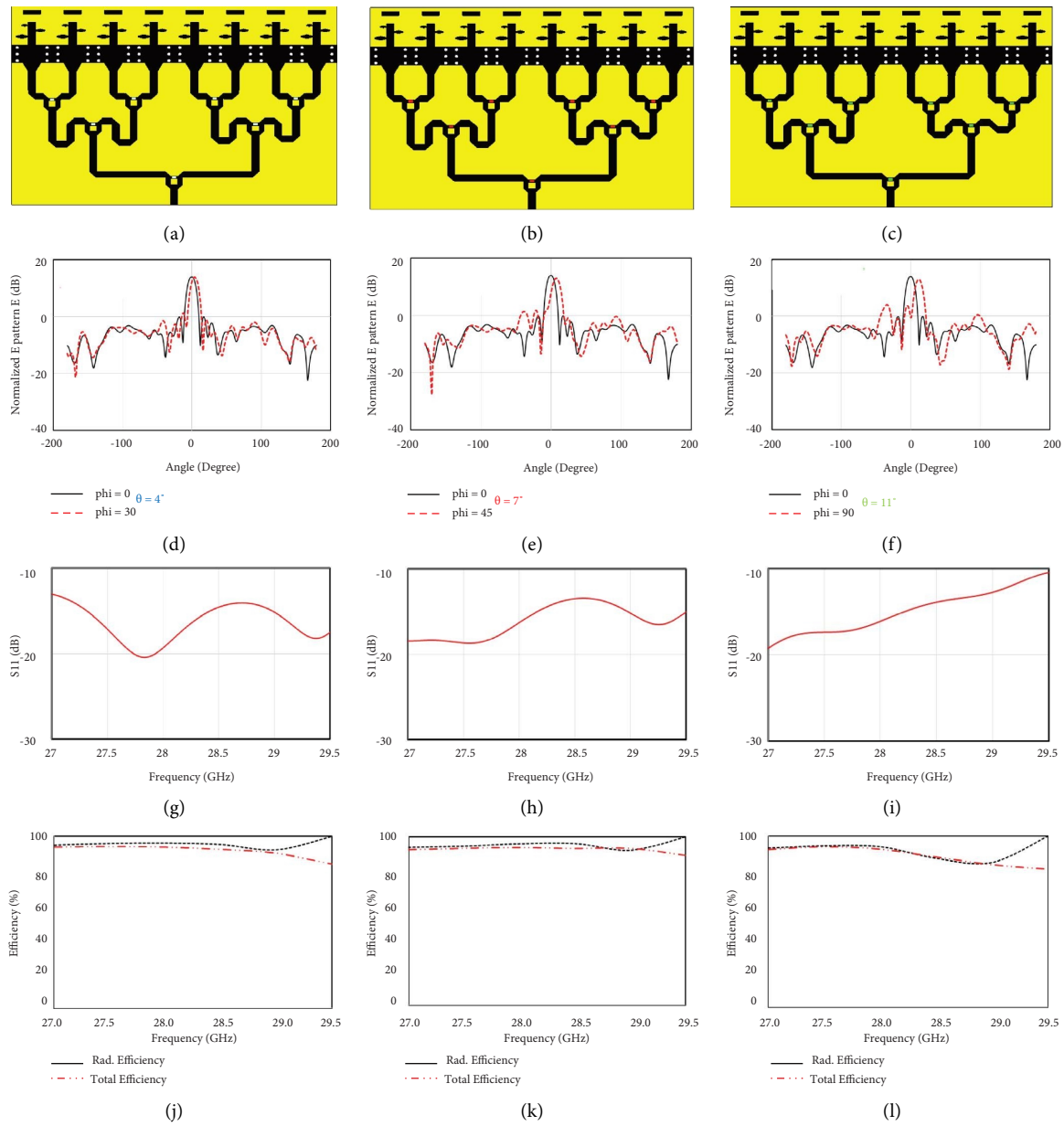

FIGURE 10: a). Phase difference 30 degree($\theta = 4^{\circ}$), d, g, j are results of normalized E – pattern with respect to 0° phase difference, S_{11} and Efficiency of this state, respectively. (b). Phase difference 45 degree($\theta = 7^{\circ}$), e, h, k are results of normalized E-pattern with respect to 0° phase difference, S_{11} and Efficiency of this state respectively. (c). Phase difference 90 degree($\theta = 11^{\circ}$), f, i, l are results of normalized E-pattern with respect to 0° phase difference, S_{11} and Efficiency of this state respectively.

To compare the simulated and calculated "θ", Table 2 is provided. From Table 2, the calculated and measured θ are very similar for various phase shifts.

5. Implementation of the Beam Switching

Because of similarity, in this part, only beam switching is designed for $\theta = 11^{\circ}$ and 11°. As Figure 11 shows switched line phase shifter technique with diodes is implemented. Phase difference is producing by changing in the length L_0 to L_3 which is calculated in Table 3 and using "on" and "off" states of diodes. From equations (13)–(17) for $\theta = 11^{\circ}$ and $\theta = -11^{\circ}$ the required phase shift is 90° and −90°, respectively.

In Figure 12(a) the overall structure of the proposed antenna is shown. The diodes used to switch and select the

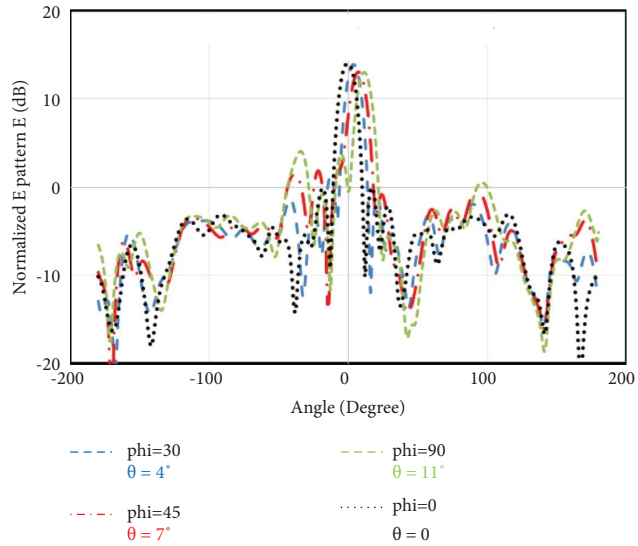

Figure 11: Normalized E patterns for various phase shifts and beam rotating.

Table 2: Simulated and calculated "θ"

φ (degree)	30°	45°	90°
θ simulated	3.94	6	11.9
θ calculated	4	7	11

Table 3: L_0 to L_3 values for $\theta = 11^\circ$ and $\theta = -11^\circ$.

φ (degree)	L_0 (mm)	L_1 (mm	L_2 (mm)	L_3 (mm)	θ (degree)
90	7.86	5.89	3.93	1.96	11.9
−90	7.86	9.825	11.79	13.775	−11.88

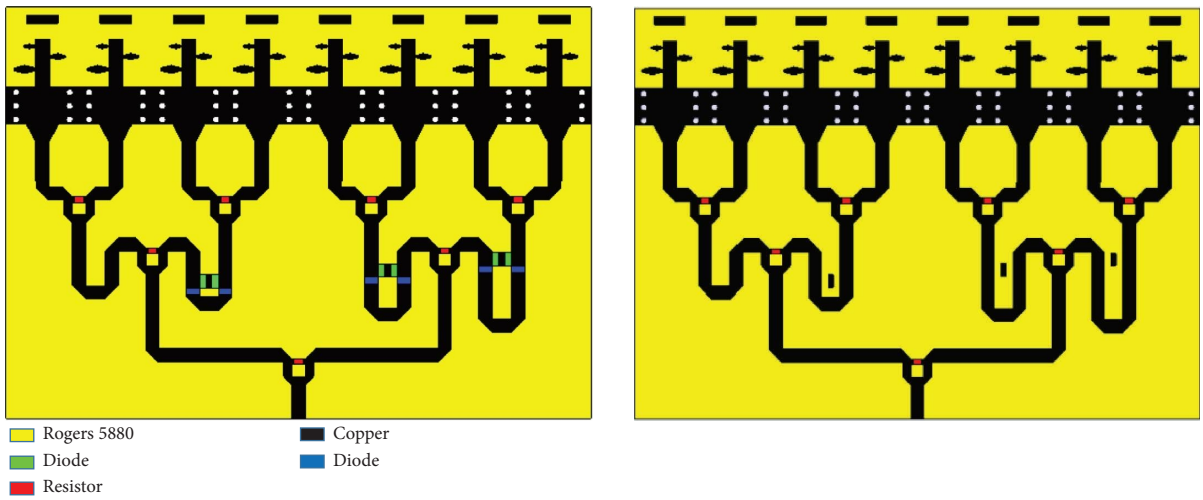

(a) (b)

Figure 12: Continued.

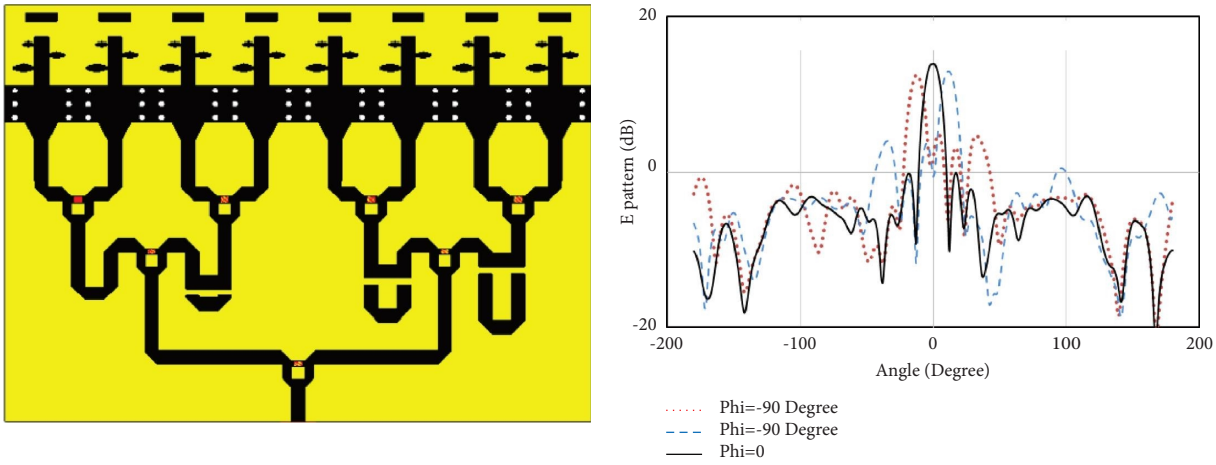

(c) (d)

FIGURE 12: (a). The linear array antenna with beam rotation ability, (b). Green diodes "on", and Blue diodes "off," (c). Green diodes "off," and Blue diodes "on," (d). the result of beam rotation for $\varphi = 90\,(\theta = 11^{\circ})$ and $\varphi = -90\,(\theta = -11^{\circ})$ degrees with respect to 0 degree.

TABLE 4: Comparison of some beam steering.

Ref. Num.	Freq.(GHz)	Gain (dB)	Radiation at $\theta = 0^{\circ}$	5G application	Size (λ_0^3)	Size reduction	Efficiency
[26]	6.59–6.69	9	Yes	No	$1.5 \times 11.58 \times 0.205$	86.2%	N.A
[27]	6.1–7.2	14–16	Yes	No	$37 \times 3.17 \times 0.579$	99.2%	65%
[28]	6.59–6.72	≈ 5	Yes	No	$1.5 \times 11.58 \times 0.205$	86.2%	N.A
[29]	6.2–6.8	7.1	Yes	No	$0.21 \times 9.34 \times 0.748$	66.66%	78.5%
[30]	27.5–28.5	8.01	Yes	Yes	$5.6 \times 12.6 \times 0.074$	90.6%	90%
[31]	25–27	10.5–12	Yes	Yes	$8.41 \times 3.73 \times 0.35$	95.5%	95.6%
[32]	28	11.62	Yes	Yes	$7.55 \times 7.55 \times 0.22$	96.1%	96.21%
This work	27–29.5	14.6	Yes	Yes	$2.8 \times 4.86 \times 0.036$	—	> 95%

paths. In Figure 12 when the green diodes are on "on" state and blue diodes are "off," $\theta = -11^{\circ}$ and When the green diodes are on "off" state and blue diodes are "on," $\theta = 11^{\circ}$.

From Figure 12 the rotation of the patterns are observed clearly. By the changing the phase difference angles and associated lengths, favorite beam steering angle (θ) can reach. But increase in the number of switches leads to increase the complexity of the design. Thus it is better to use from other beam steering methods [23–25].

Table 4 presents a comparison between some beam steering methods in various frequencies. As it can be seen from the table, the size of this work is the smallest. The structure of the proposed antenna. is planar, easy to fabrication, and integrates with other devices. In some methods [26–29] the. ferrite used which can increase the losses and size of the antenna. The small size of the antenna makes it suitable to apply in handheld devices such as cellphones, tablets, and laptops. However, the methods to create beam steering in [26–29] do not have any mechanical switches (for example microelectro-mechanical switches (MEMS), or pin diode, and varactor) which can add some losses to the system. In [30–32] the antennas have good efficiency and almost enough gain but the size of the proposed antenna in this work is smaller. Also, the proposed antenna has the required gain for 5G application (At least is 12 dB).

6. Conclusions

An end fire antenna which is planar, with compact size, lightweight, simple structure, and high gain is proposed, simulated, and fabricated. The feeding part is the Wilkinson power divider which provides an ability to beam switching by using switched line phase shifter technique. The switching action is done by "on" and "off" states of diodes which allow selecting the path of current in the transmission lines. The simulation results for the phased array antenna show that when beam switching and beam rotation is done the S_{11} coefficients, efficiency, and pattern of the antenna are acceptable. Also, the operation of the antenna is not degraded. By choosing the phase shift degree, beam direction can be changed. Thus, this type of antenna is a good candidate to mmW/5G (27–29.5 GHz) application and systems especially for handheld devices.

Data Availability

The data used to support the study are included in the paper.

Conflicts of Interest

The author declares that there are no conflicts of interest.

References

[1] V. Y. K. Loung, R. Ngah, J. Owusu, C. T. Han, S. Tweneboah-Koduah, and J. Din, "Key technologies and future trends of 5G wireless network applications," in *Proceedings of the 2021 IEEE 6th International Conference on Signal and Image Processing (ICSIP)*, July 2021.

[2] D. Fang, Y. Qian, and R. Q. Hu, "Security for 5G mobile wireless networks," *IEEE Access*, vol. 6, pp. 4850–4874, 2018.

[3] A. Tikhomirov, E. Omelyanchuk, and A. Semenova, "Recommended 5G frequency bands evaluation," in *Proceedings of the 2018 Systems of Signals Generating and Processing in the Field of on Board Communications*, April 2018.

[4] H. Kähkönen, J. Ala-Laurinaho, and V. Viikari, "Surface-mounted ka-band Vivaldi antenna array," *IEEE Open Journal of Antennas and Propagation*, vol. 2, pp. 126–137, 2021.

[5] S. Gupta, Z. Briqech and A. R. Sebak, Metamaterial-corrugated fermi tapered slot antenna for MMW applications," in *Proceedings of the 2017 IEEE International Symposium on Antennas and Propagation & USNC/URSI National Radio Science Meeting*, July 2017.

[6] M. Chen, N. Liu, W. Xue, and J. Tarng, "Compact millimeter-wave triband quasi-yagi antenna for 5G and WiGig applications," in *Proceedings of the 2019 PhotonIcs & Electromagnetics Research Symposium - Spring (PIERS-Spring)*, June 2019.

[7] L. Yang and J. J. Zhuang, ""Compact quasi-Yagi antenna with enhanced bandwidth and stable high gain"," *Electronics Letters*, 2020.

[8] C. Di Paola, Z. Ying, T. Bolin, G. F. Pedersen, S. Zhang, and K. Zhao, ""Wideband beam-switchable 28 GHzQuasi-yagi array for mobile devices"," *IEEE Transactions on Antennas and Propagation*, vol. 67, no. 11, pp. 6870–6882, 2019.

[9] S. Dinesh, C. V. Vinisha, D. D. Krishna, J. M. Laheurte, and C. K. Aanandan, "Highly directive planar end-fire antenna array," *Progress In Electromagnetics Research C*, vol. 106, pp. 45–59, 2020.

[10] O. Gassab, A. Azrar, A. Dahimene, S. Bouguerra, and C. He, ""Efficient electronic beam steering method in time modulated linear arrays"," *IET Microwaves, Antennas & Propagation*, 2018.

[11] H. J. Visser, "Antenna theory and applications," *John Wiley & Sons*, 2012.

[12] A. Lak, Z. Adelpour, H. Oraizi, and N. Parhizgar, "Three configurations of compact planar multi-stub microstrip antennas for mmW mobile application," *International Journal of Antennas and Propagation*, 2021.

[13] A. Lak, Z. Adelpour, H. Oraizi, and N. Parhizgar, ""Design and SAR assessment of three compact 5G antenna arrays"," *Scientific Reports*, vol. 11, no. 1, Article ID 21265, 2021.

[14] M. B. Jamshidi, S. Roshani, J. Talla, S. Roshani, and Z. Peroutka, "Size reduction and performance improvement of a microstrip Wilkinson power divider using a hybrid design technique," *Scientific Reports*, vol. 11, no. 1, p. 7773, 2021.

[15] Y. J. Cheng, "Substrate Integrated Antenna and Ararays," *Taylor & Francis Group, Florida, USA, 2016*, 2016.

[16] Z. N. Chen and X. Qing, "Substrate-integrated millimeter-wave antennas for next-generation communication and radar systems," *John Wiley & Sons*, 2021.

[17] H. Oraizi, A. Amini, and M Karimi Mehr, "Design of miniaturised UWB log-periodic end-fire antenna using several fractals with WLAN band-rejection," *IET Microwaves, Antennas & Propagation*, vol. 11, no. 2, pp. 193–202, 2017.

[18] K. M. Younus, A. A. Jasim, and R. W. Clarke, "A beam steering system design based on phased array antennas," in *Proceedings of the 1st International Ninevah Conference on Engineering and Technology*, Ninevah, Iraq, April 2021.

[19] P. Bhartia, I. Bahl, and R. Garg, *Ittipiboon," Micro Strip Antenna Design Handbook*, Artech House, USA, 2001.

[20] A. Chakraborty and B. Gupta, ""Paradigm phase shift: RF MEMS phase shifters: an overview"," *IEEE Microwave Magazine*, vol. 18, no. 1, pp. 22–41, 2017.

[21] A. Chakraborty and A. Kumar Kar, "MEMS-Based phase shifters for phased array applications fully integrated on PCB substrates," in *Proceedings of the International Conference on Signal, Networks, Computing, and Systems*, Springer, India, 2016.

[22] P. V. Seshadri, *"Analog Phase Shifter at X-Band Frequency"*, Anna University, 2011.

[23] M. A. Hassanien, M. Jenning, and D. Plettemeier, "beam steering system using rotman lens for 5G applications at 28 GHz," in *Proceedings of the Conference: 2017 IEEE AP-S Symposium on Antennas and Propagation, USA*, July 2017.

[24] S. Lee, Y. Lee, and H. Shin, "A 28-GHz switched-beam antenna with integrated butler matrix and switch for 5G applications," *Sensors*, 2021.

[25] A. M. Montaser and K. R. Mahmoud, ""Deep learning based antenna design and beam-steering capabilities for millimeter-wave applications"," *IEEE Access*, vol. 9, pp. 145583–145591, 2021.

[26] M. Shirkolaei and J. Ghalibafan, "Magnetically scannable slotted waveguide antenna based on the ferrite with gain enhancement," *Waves in Random and Complex Media*, 2021.

[27] M. Mohammadi, F. Hodjat Kashani, and J. Ghalibafan, "A partially ferrite-filled rectangular waveguide with CRLH response and its application to a magnetically scannable antenna," *Journal of Magnetism and Magnetic Materials*, vol. 491, p. 165551, 2019.

[28] M. Mohammadi, F. H. Kashani, and J. Ghalibafan, "Backfire-to-endfire scanning capability of a balanced metamaterial structure based on slotted ferrite-filled waveguide," *Waves in Random and Complex Media*, vol. 31, no. 6, pp. 1211–1225, 2021.

[29] M. Mohammadi Shirkolaei and J. Ghalibafan, "Scannable leaky-wave antenna based on ferrite-blade waveguide operated below the cutoff frequency," *IEEE Transactions on Magnetics*, vol. 57, no. 4, pp. 1–10, 2021.

[30] W. W. Lee, I. J. Hwang, and B. Jang, "End-fire Vivaldi antenna array with wide fan-beam for 5G mobile handsets," *IEEE Access*, vol. 8, pp. 118299–118304, 2020.

[31] N. OjaroudiParchin, M. Alibakhshikenari, H. Jahanbakhsh Basherlou, R. Abd-Alhameed, J. Rodriguez, and E. Limiti, "" MM-wave phased array Quasi-Yagi antenna for the upcoming 5G cellular communications"," *Applied Sciences*, vol. 9, no. 5, p. 978, 2019.

[32] J. Bang and J. Choi, ""A compact hemispherical beam-coverage phased array antenna unit for 5G mm-Wave applications"," *IEEE Access*, vol. 8, pp. 139715–139726, 2020.